

# A GENERALIZED CONTINUUM FORMULATION FOR COMPOSITE MICROCRACKED MATERIALS AND WAVE PROPAGATION IN A BAR

Patrizia TROVALUSCI<sup>a</sup>, Valerio VARANO<sup>b</sup>, Giuseppe REGA<sup>a</sup>

<sup>a</sup>Department of Structural Engineering and Geotechnics,  
'Sapienza' University of Rome, Via Gramsci 97, 00197 Rome, ITALY.  
E-mail: patrizia.trovalusci@uniroma1.it

<sup>b</sup>Department of Structures, University 'RomaTre', Via Segre 4/6, 00146 Rome, ITALY.

**ABSTRACT** A multifield continuum is adopted to grossly describe the dynamical behaviour of composite microcracked solids. The constitutive relations for the internal and external (inertial) actions are obtained using a multiscale modelling based on the hypotheses of the classical molecular theory of elasticity, and the ensuing overall elastodynamic properties allow us to take properly into account the microscopic features of these materials. Referring to a one-dimensional microcracked bar, the ability of such a continuum to reveal the presence of internal heterogeneities is investigated by analysing the relevant dispersive wave propagation properties. Scattering of travelling waves is shown to be associated with the microcrack density in the bar.

**Keywords:** composite materials, multifield continua, multiscale modelling, lattice mechanics, coarse-graining, wave propagation, dispersion.

## 1. INTRODUCTION

The demand for high-performance structural materials in several domains of engineering and technology calls for the need to define models for the macroscopic behaviour of complex materials that show, at finer scales, various kinds of heterogeneities. Among them are polyphase metallic alloy systems, polymer blends, polycrystalline, porous or textured media, fibre-matrix composites, bio-composites, and masonry-like or jointed materials. Such improved materials are classified as complex due to both the presence of complex internal microstructures and their constitutive behaviour. The ability to design such materials and to derive their macroscopic properties relies, in turn, on the ability to take into account the internal structure, size, shape, spatial distribution of the microstructural constituents which can span several orders of magnitude in length, starting from the submicron scale to mm or even larger scales. Analogous demands concern in fact both materials with random microstructures and traditional composites such as masonry-like materials with periodic mesostructures.

A basic problem in the mechanical modelling of such complex materials is the identification of suitable constitutive laws able to take into account the microscopic features avoiding a direct modelling of the microstructure, whose discretization can lead to cumbersome problems with many degrees of freedom [1]-[3]. Since many years several homogenization or coarse-graining methods have been introduced to deal with a multiscale phenomenology [4], [5], and also with material randomness, which requires the accurate definition of the domain

sizes involved in the micro-macro transition process [6], [7]. While such methods have been quite successful at describing the global response of non-linear composite materials [8], [9], even if formulated in a deterministic framework, most of classical “homogenized” models are standard continua that exhibit two major drawbacks. First, lacking on material internal scale parameters, they cannot predict the effect of the size and orientation of the heterogeneities, since they account only for shape factors of internal phases and, in some cases, for the morphology of the heterophase distribution [10]-[12]. Second, they generally assume the local macroscopic uniformity of the stress-strain fields, which is likely to be inappropriate in critical regions of high gradients, e.g. in the vicinity of a macroscopic discontinuity such as a joint or a hole, or close to the point of application of a localized load [13], [14]. The main difficulties arise when the characteristic size of the problem under consideration is of the same order of magnitude as the size of the internal heterogeneities. Moreover, when non-linear and non-monotone stress-strain laws are involved, such difficulties increase. In this case, ill-posedness of the field equations as well as strongly mesh-dependency in the numerical solutions may arise [15], [16]. Several models have tried to overcome such difficulties by introducing non-simple Cauchy continua, such as the strain gradient or non-local models [17], [18]. In all these models non-standard strain measures, implying spatial derivatives of order different than the second in the equations of motion, are involved in order to make the problem well posed. However, thermodynamic inconsistency arises because no stress measures correspond, in the sense of the virtual work, to these additional strain measures [19]. Models intrinsically free from the above limitations have been also developed within the framework of micromorphic materials [8]-[10], [20]-[23].

In the present paper we generalize a multiscale approach first formulated in [24], [25] and used, [26]-[28], to grossly describe the mechanical behaviour of composite media made of short, stiff and strong fibres embedded in a more deformable matrix which, due to manufacturing defects or lack of cohesion, presents distributed micro-flaws, thereby providing an accurate description of the microstructure with a convenient computational cost with respect to conventional homogenization techniques (e.g. [4]). This approach relates macroscopic deformations of continua to changes in positions and other parameters describing the material microstructure, of specific lattice models. It is based on the assumptions of the molecular/energetic theory of elasticity originally formulated by Voigt and Poincaré [29]-[31] and further developed also to account for non-linear and non-local effects (see [32]) in the first works on continuum micromechanics [33]-[35] and in more recent atomistic-continuum models for complex materials [36]-[39] or even in graph-theoretic, energy-based, homogenized continua for granular media [40]. The energy equivalent continuous models derived in such a way naturally belong to the class of multifield continuous models [40]-[43] characterized by the presence of more field descriptors than the classical continuum, which allow to retain ‘memory’ of the fine organization of the materials. For such continua the basic starting point is to consider the generic material patch as a system and to introduce information on the material microstructure, already at the geometrical level of the body description. The material patch is then characterized not only by its spatial position but also by suitable field descriptors of the microstructural morphology which are associated to interactions that satisfy suitable balance equations and pose nontrivial constitutive problems.

The multiscale approach here adopted starts from the description of the material at the level of the microstructure (fibres and microcracks) and uses a virtual work equivalence procedure to derive the macroscopic constitutive description of a multifield continuum characterised by three kinematical descriptors: the standard displacement field, the so-called microdisplacement field and the microrotation field. The two non-standard fields respectively account for the presence of microcracks and fibres. The role of such additional fields is to

effectively smear the microscopic heterogeneities (microcracks and fibres, respectively) in the macroscopic continuum, allowing at the same time the introduction of material length scales (the size of the heterogeneities with respect to the leading dimension of the macroscopic system), besides the fibre and microcrack densities and aspect ratios which can also be present in the conventional Cauchy continuum.

The ability of such multiscale-multifield continuum to reveal the presence of the material microstructure is here investigated by studying wave propagation in a one-dimensional system describing a fibre-reinforced material with a microcracked elastic matrix. In particular, it is shown that the additional microstructural field descriptors make the equations of motion dispersive, with phase-velocities changing with frequency. Due to these dispersion properties, the model shows to be able to describe changes in shape of travelling waves generally associated with scattering. The case in which the microstructural relaxation does not influence the macroscopic displacement field (uncoupled model) is also discussed against the more general case in which appropriate coupled boundary conditions describe the interaction between macro and microstructure (coupled model).

The paper is organized as follows. Based on a generalized “molecular” formulation for multiscale models, a multifield continuum (macromodel) able to account for the mechanical features of an underlying fibre-reinforced microcracked composite (micromodel) is built up. In Section 2 the constitutive functions for the internal and external (inertial) actions are identified via a virtual work equivalence procedure, by referring to an internally constrained (simplified) micromodel. The balance equations of the multifield continuum are given in Section 3. Attention is then focused on the uncoupled one-dimensional model of a microcracked bar, for which free or forced wave propagation is addressed (Section 4). In the forced case, coupling between micro and macro motions is indirectly taken into account through proper boundary conditions, and the amplitude and shape features of travelling waves in variably damaged bars are investigated via multifield finite element simulations. The paper ends with some conclusions.

## 2. A ‘MOLECULAR’ FORMULATION FOR A MULTISCALE-MULTIFIELD MODEL

The continuous model of the generalised homogeneous material (macromodel) is built based on the kinematics of proper lattice models (micromodel) of the kind introduced in [24].

For the sake of clarity, our reference material is a fibre-reinforced microcracked composite, which could be a ductile polymer composite with long carbon fibres as well as a masonry-like material with stone/bricks embedded in a mortar matrix, both with a distribution of slit microcavities in the matrix. At the microscopic level such a material is described by two interacting lattice systems. One lattice, made of rigid particles of given shape, representing the fibres in the matrix and the other lattice, made of interacting slits of arbitrary shape with a predominant dimension, representing the microcracks. The two sublattices are linked together by elastic bonds.

Assuming the material microstructure as periodic, or at least statistically homogeneous, a representative volume element, here referred to as a *module*, can be defined (Fig. 1).<sup>1</sup> The procedure governing the scale transition between the micromodel and the macromodel is based on the following key assumptions.

---

<sup>1</sup> Our model refers to materials with a periodic microstructure and is developed within a purely mechanical deterministic framework, tacitly assuming an RVE with a given size. A scale-dependent homogenization should be involved if randomness were taken into account [6].

- (i) A correspondence between the set of lattice degrees of freedom and a suitable number of kinematical vector fields, representing the material internal structure, is assumed ‘a priori’. In particular, homogeneous deformations are imposed to the module.
- (ii) The volume average of the work of the internal actions of the module is equated, through the localization theorem, to the work density of the internal actions of the continuum, for any corresponding set of admissible displacements.
- (iii) The work of the external actions of the micro and macro model is equated, for any corresponding set of admissible displacements.

These hypotheses are related to basic assumptions of the classical molecular theory of elasticity, as originally delineated in the basic work by Voigt based on crystal elasticity [31] and recovered in the more recent literature [32]. Namely, the hypothesis (i) can be reduced to the so-called Cauchy-Born hypothesis [44], [45] while hypotheses (ii) and (iii) are standard in energy-based homogenization approaches, in particular the former is related to the energy averaging theorem known in literature as the Hill-Mandel condition [46]. All of these hypotheses are generally employed in coarse-graining models based on lattice descriptions [33]-[39].

Overall, with respect to previous authors’ papers [24], [28] addressing the same problem based on variable – and possibly limiting – assumptions, the micro-macro identification is herein pursued:

(i) by considering a generalized approach based on the virtual work equivalence, which allows to identify stress measures of the macromodel without a priori specifying the constitutive functions for the internal actions of the micromodel, as it would occur when pursuing an energy-based equivalence [28];

(ii) by taking into account the full interaction between the two lattice systems of the micromodel, as well as the inertial actions, in contrast to [24]; this is properly reflected into a fully coupled generalized (multifield) macromodel.

Further specific differences arising in the identification procedure with respect to previously formulated macromodels will be highlighted in the sequel.

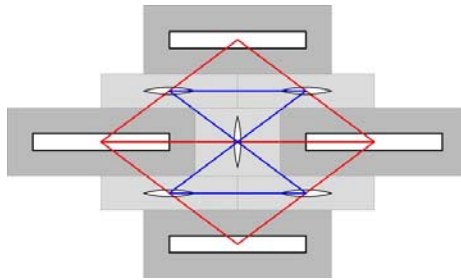


**Figure 1.** An orthotropic module with particles, slits and relevant mass portions. For the sake of simplicity, one slit for each pair of particles is represented.

## 2.1. The micro-model: a Lagrangian description

The lattice model is a system made of interacting rigid particles, representing the fibres, and deformable slits, representing the microcracks, located in between the particles. In the considered reference material the size of the particles is larger than the slit size. Accordingly, only particles are given an orientation, namely, we assume beam-like interactions between pairs of particles and truss-like interactions between pairs of slits. Beam-like interactions also hold

for the mixed particle-slit pairs. In addition, taking into account only short-range interactions allows us to consider linearized kinematics.

The kinematical descriptors of the system are the displacement of the centre  $\mathbf{a}$  of each particle  $A$ , represented by the vector  $\mathbf{u}^a$ , and the particle rotation, represented by the skew-symmetric tensor  $\mathbf{W}^a$ . Moreover, as independent kinematical descriptors of a slit  $H$  we assume the vector  $\mathbf{u}_p^h$ , representing the displacement of a point  $\mathbf{p}^h$  of the slit, and the vector  $\mathbf{d}^h$ , representing the crack-opening displacement over  $H$ , being  $\mathbf{h}$  the centre of the slit (Fig. 2).

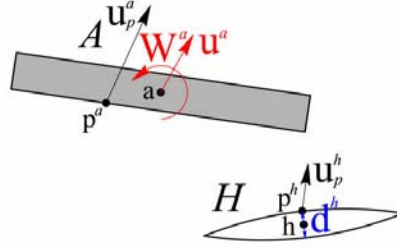


**Figure 2.** Lattice kinematical descriptors.

As strain measures of the assembly we assume the relative displacement between two points,  $\mathbf{p}^a$  and  $\mathbf{p}^b$  respectively selected on the particles  $A$  and  $B$ ,  $\mathbf{u}^{ab} = \mathbf{u}_p^a - \mathbf{u}_p^b = [\mathbf{u}^a + \mathbf{W}^a(\mathbf{p}^a - \mathbf{a})] - [\mathbf{u}^b + \mathbf{W}^b(\mathbf{p}^b - \mathbf{b})]$  and the relative rotation between  $A$  and  $B$ ,  $\mathbf{W}^{ab} = \mathbf{W}^a - \mathbf{W}^b$ . Additional strain measures are the displacement jump,  $\mathbf{d}^h$ , and the relative displacement jump,  $\mathbf{d}^{hk} = \mathbf{d}^h - \mathbf{d}^k$ , between two interacting slits  $H$  and  $K$ . For each pair of interacting particle-slit, a further strain measure is assumed as the vector  $\mathbf{u}^{ah} = \mathbf{u}_p^a - (\mathbf{u}_p^h + \alpha^h \mathbf{d}^h)$ , being  $\alpha^h$  a non negative coefficient depending on  $\|\mathbf{p}^a - \mathbf{p}^h\|$  and on the number of particles interacting with  $H$ .

The particles are subjected to forces and couples, respectively represented by the vector  $\mathbf{f}^a$ , and the skew-symmetric tensor  $\mathbf{M}^a$ , while no external forces are applied to the slits. Denoting with  $\rho^a$  the mass of a particle plus the relevant portion of the matrix and with  $\rho^h$  the relevant mass of a slit  $H$  (Fig. 1), the inertial forces  $\rho^a \ddot{\mathbf{u}}^a$  and couples  $\mathbf{A}^a$  act on the particles as well as the inertial forces  $\rho^h \ddot{\mathbf{u}}_p^h$  and  $\rho^h \ddot{\mathbf{d}}^h$  act on the slits. The skew-symmetric tensor  $\mathbf{A}^a$  is the time derivative of the angular momentum,  $\mathbf{A}^a = \mathbf{E}^a (\dot{\mathbf{W}}^a + \mathbf{W}^{a^2})^T - (\dot{\mathbf{W}}^a + \mathbf{W}^{a^2}) \mathbf{E}^a$ , and  $\mathbf{E}^a$  is the Euler tensor of the particle  $A$ .<sup>2</sup>

The actions that a particle  $B$  ( $A$ ) exerts on a particle  $A$  ( $B$ ), through  $\mathbf{p}^a$  and  $\mathbf{p}^b$ , are represented by the vector of forces  $\mathbf{t}^a$  ( $\mathbf{t}^b$ ) and the skew-symmetric tensor of couples  $\mathbf{C}^a$  ( $\mathbf{C}^b$ ); the vector  $\mathbf{z}_0^h$  represents the crack-opening force over a slit  $H$  ( $K$ ); the vector  $\mathbf{z}^h$  ( $\mathbf{z}^k$ ) represents the force that a slit  $K$  ( $H$ ) exerts on a slit  $H$  ( $K$ ), while the vector  $\mathbf{r}^a$  ( $\mathbf{r}^h$ ) represents the force that  $H$  ( $A$ ) exerts on  $A$  ( $H$ ), through  $\mathbf{p}^a$  and  $\mathbf{p}^h$  (Fig. 3).

<sup>2</sup> Dot symbol indicates the time derivative of a variable.

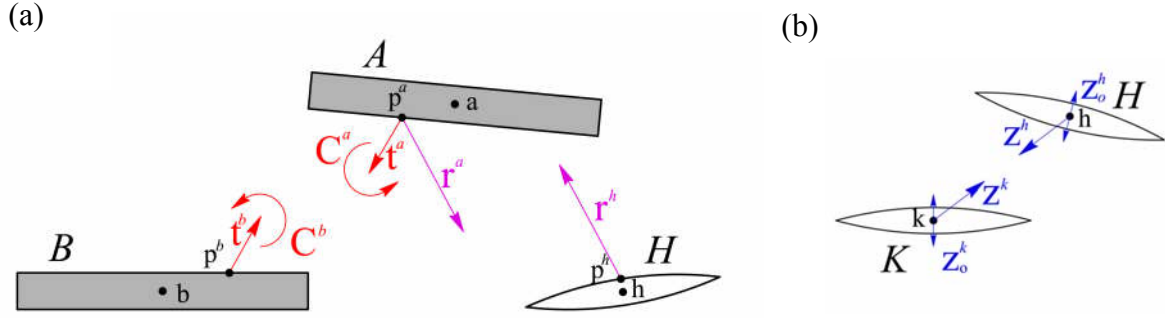


**Figure 3.** Lattice statical interactions: (a) particle-particle, slit-particle, (b) slit-slit. The equilibrium equations for each particle  $A$  and each slit  $H$  of the system can be written as<sup>3</sup>

$$\begin{aligned}
 \sum_{i=1}^{N_a} \mathbf{t}_i^a + \sum_{l=1}^{L_a} \mathbf{r}_l^a &= \mathbf{f}^a - \rho^a \ddot{\mathbf{u}}^a, \\
 \sum_{i=1}^{N_a} \left\{ \mathbf{C}_i^a + \frac{1}{2} [(\mathbf{p}_i^a - \mathbf{a}) \otimes \mathbf{t}_i^a - \mathbf{t}_i^a \otimes (\mathbf{p}_i^a - \mathbf{a})] \right\} + \sum_{l=1}^{L_a} \frac{1}{2} [(\mathbf{p}_l^a - \mathbf{a}) \otimes \mathbf{r}_l^a - \mathbf{r}_l^a \otimes (\mathbf{p}_l^a - \mathbf{a})] &= \mathbf{M}^a - \mathbf{A}^a, \\
 \sum_{j=1}^{M_h} \mathbf{z}_j^h + \sum_{l=1}^{L_h} \mathbf{r}_l^h + \mathbf{z}_o^h &= -\rho^h \dot{\mathbf{d}}^h - \rho^h \ddot{\mathbf{u}}_p^h,
 \end{aligned} \tag{1}$$

where  $N_a$  is the number of particles interacting with the particle  $A$ ,  $M_h$  is the number of slits interacting with the slit  $H$ ,  $L_a$  is the number of slits interacting with the particle  $A$  and  $L_h$  is the number of particles interacting with the slit  $H$ . Moreover, the balance of internal actions of the module gives

$$\begin{aligned}
 \mathbf{t}^a + \mathbf{t}^b &= \mathbf{0}, \\
 \mathbf{z}^h + \mathbf{z}^k &= \mathbf{0}, \\
 \mathbf{r}^a + \mathbf{r}^h &= \mathbf{0}, \\
 \mathbf{C}^a + \mathbf{C}^b + \frac{1}{2} \{ [(\mathbf{p}^b - \mathbf{p}^a) \otimes \mathbf{t}^b - \mathbf{t}^b \otimes (\mathbf{p}^b - \mathbf{p}^a)] + \sum_{l=1}^{L_{ab}} [(\mathbf{p}_l^h - \mathbf{p}^a) \otimes \mathbf{r}_l^h - \mathbf{r}_l^h \otimes (\mathbf{p}_l^h - \mathbf{p}^a)] \} &= \mathbf{0}.
 \end{aligned} \tag{2}$$

for each pair of particles ( $A$ ,  $B$ ), slits ( $H$ ,  $K$ ), particle-slits ( $A$ ,  $H$ ), and triplet ( $AHB$ ), respectively.  $L_{ab}$  is the number of slits located in between  $A$  and  $B$ .<sup>4</sup>

<sup>3</sup> We use the representation of infinitesimal rotations and moments through skew-symmetric tensors instead of axial vectors. It is worth noting that there exists a one-to-one relation between the two notations:  $\Theta \mathbf{v} = \Theta \times \mathbf{v}$ ,  $\forall \mathbf{v} \in \mathcal{V}$ , where  $\Theta$  is a skew-symmetric tensor,  $\Theta$  is its axial vector and  $\mathcal{V}$  is a vector space.

<sup>4</sup> The beam-like interactions between particle-slits entail a multiple interaction ( $AHB$ ) in the moment balance equations. Of course, various kinds of interactions can be considered but with the assumed no-central force scheme, in analogy to the Voigt and Poincaré approaches to molecular linear elasticity, we expect to identify a correct number of material constants [32]. Moreover, this assumption will allow us to identify a symmetric macro stress tensor.

Let us now consider the representative volume element referred to as the ‘module’. The module volume  $V$  is defined as the sum of elementary volumes attributed to particles and slits.<sup>5</sup> Taking into account Eqs. (1)-(2), and putting

$$\mathbf{t}^a = -\mathbf{t}^b = \mathbf{t}^{ab}, \quad \mathbf{z}^h = -\mathbf{z}^k = \mathbf{z}^{hk}, \quad \mathbf{r}^a = -\mathbf{r}^h = \mathbf{r}^{ah},$$

$$\mathbf{C}^a = \{[\mathbf{t}^{ab} \otimes (\mathbf{p}^a - \mathbf{p}^b) - (\mathbf{p}^a - \mathbf{p}^b) \otimes \mathbf{t}^{ab}] + \sum_{l=1}^{L_{ab}} [\mathbf{r}_l^{ah} \otimes (\mathbf{p}^a - \mathbf{p}^h) - (\mathbf{p}^a - \mathbf{p}^h) \otimes \mathbf{r}_l^{ah}]\} / 2 - \mathbf{C}^b = \mathbf{C}^{ab},$$

the mean work (micro-work) of the internal actions of the module can be expressed as follows

$$\bar{w}_\mu^i = \frac{1}{V} \left\{ \sum_{ab} \mathbf{t}^{ab} \cdot [\mathbf{u}^{ab} - \mathbf{W}^a (\mathbf{p}^a - \mathbf{p}^b)] + \frac{1}{2} \mathbf{C}^{ab} \cdot \mathbf{W}^{ab} \right. \\ \left. + \sum_h \mathbf{z}_0^h \cdot \mathbf{d}^h + \sum_{hk} \mathbf{z}^{hk} \cdot \mathbf{d}^{hk} + \sum_{ah} \mathbf{r}^{ah} \cdot [\mathbf{u}^{ah} - \mathbf{W}^a (\mathbf{p}^a - \mathbf{p}^h)] \right\}, \quad (3)$$

where the summations on  $ab$ ,  $hk$ ,  $ah$  range, respectively, from 1 to the number of the pair of particles, slits and particle-slits in the module, while the summation on  $h$  ranges from 1 to the number of slits. In turn, the mean (micro) work of the external (inertial and non inertial) actions over the module can be expressed as

$$\bar{w}_\mu^e = \frac{1}{V} \left\{ \sum_a [\mathbf{f}^a \cdot \mathbf{u}^a - \rho^a \ddot{\mathbf{u}}^a \cdot \mathbf{u}^a + \frac{1}{2} (\mathbf{M}^a \cdot \mathbf{W}^a - \mathbf{A}^a \cdot \mathbf{W}^a)] - \sum_h \rho^h (\ddot{\mathbf{u}}_p^h \cdot \mathbf{u}_p^h + \ddot{\mathbf{d}}^h \cdot \mathbf{d}^h) \right\}, \quad (4)$$

where the summations on  $a$  and  $h$  range from 1 to the number of particles and slits of the module, respectively.<sup>6</sup>

As response functions for the particle interactions,  $\mathbf{t}^{ab}$  and  $\mathbf{C}^{ab}$ , as well as for the opening force on slits,  $\mathbf{z}_0^h$ , we assume linear elastic constitutive laws while we consider non-linear elastic laws for the slit-slit force,  $\mathbf{z}^{hk}$ , and the particle-slit force,  $\mathbf{r}^{ah}$ ,

$$\mathbf{t}^{ab} = \mathbf{K}^{ab} [\mathbf{u}^{ab} - \mathbf{W}^a (\mathbf{p}^a - \mathbf{p}^b)], \quad \mathbf{C}^{ab} = \mathbf{K}^{ab} \mathbf{W}^{ab},$$

$$\mathbf{z}_0^h = \mathbf{D}^h \mathbf{d}^h, \quad \mathbf{z}^{hk} = D^{hk} \left| \mathbf{d}^h \right| \left| \mathbf{d}^k \right| \frac{\mathbf{h} - \mathbf{k}}{|\mathbf{h} - \mathbf{k}|^2}, \quad \mathbf{r}^{ah} = \frac{f_1(\mathbf{p}^a) f_2(\mathbf{p}^h)}{|\mathbf{p}^a - \mathbf{p}^h|^2}. \quad (5)$$

In Eqs. (5)  $\mathbf{K}^{ab}$  and  $\mathbf{K}^{ab}$  are symmetric constitutive tensors of the second and fourth order containing the stiffness and rotational stiffness terms, respectively. Since we assume the fibres as rigid, these terms depend on the elastic constants of the matrix and on the geometry of the module.  $\mathbf{D}^h$  is a symmetric second order tensor defining the ‘‘microcrack-stiffness’’, which also depends on the elastic constants of the matrix and on the geometry of the module. The constitutive function for the interactions between slits,  $\mathbf{z}^{hk}$ , is assumed analogous to the interacting function between parallel edge dislocations, supposing each slit  $H$  as a continuous distribution of edge dislocations having the microcrack jump  $|\mathbf{d}^h|$  as Burger’s vector [47];  $D^{hk}$  is a constant depending on the elastic constants of the matrix and the microcrack size [25].

<sup>5</sup> Note that this definition could be refined by distinguishing between the different elementary volumes of the lattice elements, as in rigorous Voronoi tessellations of atomistic models of matter [39].

<sup>6</sup> In the following the same symbols in the summations indicate the same ranges for indexes.

Finally, for the non-linear interactions between slits and particles,  $\mathbf{r}^{ah}$ , we consider a phenomenological relation between microcracks and hard fibres embedded in an elastic matrix of silicon carbide, of the kind proposed in [48], with  $f_1$  and  $f_2$  being two approximately Gaussian functions describing the local force field around a particle  $A$  and a slit  $H$ , respectively.

It is worth noting that at this stage Eqs. (5) are only paradigmatic of the multiscale perspective in which all the interaction laws of the microscopic model can be defined at different scale levels, such as mesoscale or micro/atomic-scale levels. In this framework the physics of the micro-model can be modified to better agree with experience, while the transition procedure between micro and macro scale is invariant.

## 2.2. Micro-macro scale transition procedure for a constrained model

To derive the constitutive equations for the internal actions of the macromodel we follow an approach originally proposed in [24] and referable to the approach by Voigt, [29] [31], who conciliated the point of view of the classical molecular theory of elasticity, by Navier, Cauchy and Poisson, with the potential theory by Green. Herein, such a multiscale approach is extended for deriving the constitutive functions for the inertial actions of the macromodel.

In order to identify the constitutive functions for the internal and external actions, we assume to replace the module with a neighbourhood,  $\mathcal{M}$ , of a continuum centred at the position  $\mathbf{x}$ . Moreover, since we will identify constitutive relations accounting for only first neighbouring interactions, only homogeneous deformations are considered.

### 2.2.1. Identification of the constitutive equations

With the assumption of homogeneous deformations (hyp.  $i$ ), one has

$$\begin{aligned}\mathbf{u}^a &= \mathbf{u}(\mathbf{x}) + \nabla \mathbf{u}(\mathbf{x})(\mathbf{a} - \mathbf{x}) , & \mathbf{a} &= \mathbf{a}, \mathbf{p}^h , \\ \mathbf{W}^a &= \mathbf{W}(\mathbf{x}) + \nabla \mathbf{W}(\mathbf{x})(\mathbf{a} - \mathbf{x}) , \\ \mathbf{d}^h &= \mathbf{d}(\mathbf{x}) + \nabla \mathbf{d}(\mathbf{x})(\mathbf{h} - \mathbf{x}) .\end{aligned}\tag{6}$$

for each particle  $A$  and each slit  $H$  of the module.

In Eqs. (6)  $\mathbf{u}(\mathbf{x})$ ,  $\mathbf{W}(\mathbf{x})$  and  $\mathbf{d}(\mathbf{x})$  are regular fields linearized in a continuum neighbourhood of centre  $\mathbf{x}$ . These fields correspond, respectively, to the standard displacement vector field, a local rotation (microrotation) tensor field (skew-symmetric), and a microdisplacement vector field. The additional microscopic fields,  $\mathbf{W}(\mathbf{x})$  and  $\mathbf{d}(\mathbf{x})$ , respectively account for the rotations of the individual fibres and for the distributed displacement jump due to the presence of microflaws in the matrix.

We obtain a simplified description by postulating, according to Voigt, that the particles of the module undergo the same rotation in such a way that

$$\mathbf{W}^a = \mathbf{W}(\mathbf{x}) = \frac{1}{2}[\nabla \mathbf{u}(\mathbf{x}) - \nabla^T \mathbf{u}(\mathbf{x})] ,\tag{7}$$

for each particle  $A$  of the module. This hypothesis physically corresponds to consider fibres with the same local rigid rotation. Taking into account Eqs. (6) with the internal constraint (7), and considering that  $(\mathbf{p}^a - \mathbf{a}) = (\mathbf{p}^a - \mathbf{p}^h) - (\mathbf{a} - \mathbf{p}^h)$ , we have

$$\begin{aligned}
\mathbf{u}^{ab} - \mathbf{W}^a(\mathbf{p}^a - \mathbf{p}^b) &= [\nabla \mathbf{u}(\mathbf{x}) - \mathbf{W}(\mathbf{x})](\mathbf{a} - \mathbf{b}) = \mathbf{E}(\mathbf{x})(\mathbf{a} - \mathbf{b}), \\
\mathbf{d}^h &= \mathbf{d}(\mathbf{x}) + \nabla \mathbf{d}(\mathbf{x})(\mathbf{h} - \mathbf{x}), \\
\mathbf{d}^{hk} &= \nabla \mathbf{d}(\mathbf{x})(\mathbf{h} - \mathbf{k}), \\
\mathbf{u}^{ah} - \mathbf{W}^a(\mathbf{p}^a - \mathbf{p}^h) &= \mathbf{E}(\mathbf{x})(\mathbf{a} - \mathbf{p}^h) - \alpha^h [\mathbf{d}(\mathbf{x}) - \nabla \mathbf{d}(\mathbf{x})(\mathbf{p}^h - \mathbf{x})],
\end{aligned} \tag{8}$$

where  $\mathbf{E}(\mathbf{x}) = [\nabla \mathbf{u}(\mathbf{x}) + \nabla^T \mathbf{u}(\mathbf{x})] / 2$ . Then after some algebra, the mean work of the internal actions of the module, Eq. (3), can be written in terms of the continuum deformation fields  $\mathbf{E}$ ,  $\mathbf{d}$  and  $\nabla \mathbf{d}$ :<sup>7</sup>

$$\begin{aligned}
\bar{\mathcal{W}}_\mu^i(\mathbf{E}, \mathbf{d}, \nabla \mathbf{d}) &= \frac{1}{V} \{ [\sum_{ab} \mathbf{t}^{ab} \otimes (\mathbf{a} - \mathbf{b}) + \sum_{ah} \mathbf{r}^{ah} \otimes (\mathbf{a} - \mathbf{p}^h)] \cdot \mathbf{E} \\
&\quad + [\sum_h \mathbf{z}_0^h - \sum_{ah} \alpha^h \mathbf{r}^{ah}] \cdot \mathbf{d} + [\sum_{hk} \mathbf{z}^{hk} \otimes (\mathbf{h} - \mathbf{k}) - \sum_{ah} \alpha^h \mathbf{r}^{ah} \otimes (\mathbf{p}^h - \mathbf{x})] \cdot \nabla \mathbf{d} \}, \\
&= \mathbf{S}_\mu \cdot \mathbf{E} + \mathbf{z}_\mu \cdot \mathbf{d} + \mathbf{Z}_\mu \cdot \nabla \mathbf{d}
\end{aligned} \tag{9}$$

where

$$\begin{aligned}
\mathbf{S}_\mu &= \frac{1}{2V} \{ \sum_{ab} [\mathbf{t}^{ab} \otimes (\mathbf{a} - \mathbf{b}) + (\mathbf{a} - \mathbf{b}) \otimes \mathbf{t}^{ab}] + \sum_{ah} [\mathbf{r}^{ah} \otimes (\mathbf{a} - \mathbf{p}^h) + (\mathbf{a} - \mathbf{p}^h) \otimes \mathbf{r}^{ah}] \}, \\
\mathbf{z}_\mu &= \frac{1}{V} \{ \sum_h \mathbf{z}_0^h - \sum_{ah} \alpha^h \mathbf{r}^{ah} \}, \\
\mathbf{Z}_\mu &= \frac{1}{V} \{ \sum_{hk} \mathbf{z}^{hk} \otimes (\mathbf{h} - \mathbf{k}) + \sum_h \mathbf{z}_0^h \otimes (\mathbf{h} - \mathbf{x}) - \sum_{ah} \alpha^h \mathbf{r}^{ah} \otimes (\mathbf{p}^h - \mathbf{x}) \},
\end{aligned} \tag{10}$$

and where the ‘ $\mu$ ’ lower suffix stands for ‘micro’ quantities.

To derive continuum field quantities from discrete quantities we assume, through the localization theorem, that the mean internal work (micro) of the module, replaced by  $\mathcal{M}$ , coincides with the internal work density (macro) per unit volume,  $\boldsymbol{\omega}_M^i(\mathbf{x})$ , of a multifield continuum in any corresponding field  $\mathbf{E}$ ,  $\mathbf{d}$ ,  $\nabla \mathbf{d}$ :<sup>8</sup>

$$\bar{\mathcal{W}}_\mu^i(\mathbf{E}, \mathbf{d}, \nabla \mathbf{d}) := \lim_{\delta \rightarrow 0} \frac{1}{V(N_\delta)} \int_{N_\delta} \boldsymbol{\omega}_M^i dV = \boldsymbol{\omega}_M^i(\mathbf{x}) = \mathbf{S}_M \cdot \mathbf{E} + \mathbf{z}_M \cdot \mathbf{d} + \mathbf{Z}_M \cdot \nabla \mathbf{d} \tag{11}$$

where  $N_\delta$  is a closed ball of radius  $\delta$ , centre  $\mathbf{x}$  and volume  $V(N_\delta)$  and the ‘M’ lower suffix stands for ‘macro’ quantities.<sup>9</sup>

The quantities  $\{\mathbf{S}_M, \mathbf{z}_M, \mathbf{Z}_M\}$  have the meaning of generalized stress fields of the constrained multiscale-multifield continuum. The explicit definition of these stress measures can be obtained from the identification  $\mathbf{S}_M = \mathbf{S}_\mu$ ,  $\mathbf{z}_M = \mathbf{z}_\mu$ ,  $\mathbf{Z}_M = \mathbf{Z}_\mu$ , through Eqs. (10). It is worth noting that the identification of the stress measures via the virtual works equivalence

<sup>7</sup> From now on, the dependence of the fields on the position  $\mathbf{x}$  will be undertaken.

<sup>8</sup> The circumstance of having the symmetric part of the displacement gradient in the generalized internal work formula depends on the internal constraint (7).

<sup>9</sup> Such an assumption agrees with the standard assumptions of continuum theories based on lattice mechanics [33]-[35].

procedure does not depend on the particular choice of response functions for the internal actions of the micro-model.<sup>10</sup>

After assuming constitutive laws for the interactions of the module, in this case Eqs. (5), and by substituting into these equations Eqs. (6) and (7), the continuum stress-strain relationships can be obtained in the form

$$\begin{aligned}\mathbf{S}_M &= \mathbf{A} \mathbf{E} + \mathbf{C} \mathbf{d} + \mathbf{D} \nabla \mathbf{d} + \Psi_s \\ \mathbf{z}_M &= \mathbf{I} \mathbf{E} + \mathbf{M} \mathbf{d} + \mathbf{N} \nabla \mathbf{d} + \Psi_z \\ \mathbf{Z}_M &= \mathbf{O} \mathbf{E} + \mathbf{Q} \mathbf{d} + \mathbf{R} \nabla \mathbf{d} + \Psi_z .\end{aligned}\quad (12)$$

In the above equations the elastic tensors  $\mathbf{A}$ ,  $\mathbf{C}$ ,  $\mathbf{D}$ ,  $\mathbf{I}$ ,  $\mathbf{M}$ ,  $\mathbf{N}$ ,  $\mathbf{O}$ ,  $\mathbf{Q}$ ,  $\mathbf{R}$  depend on the elastic constants of the matrix and on the shape and the arrangement of the internal phases. The tensors  $\mathbf{C}$ ,  $\mathbf{I}$ ,  $\mathbf{M}$ ,  $\mathbf{N}$ ,  $\mathbf{Q}$  have components also depending on the size of the heterogeneities.  $\Psi_s$ ,  $\Psi_z$  and  $\Psi_z$  are non-linear functions of  $\nabla \mathbf{u}$ ,  $\mathbf{d}$  and  $\nabla \mathbf{d}$  accounting for the particle-slit and slit-slit interactions and depending on the relevant positions and orientations.

Assuming the material to be hyperelastic and taking into account linearized forces only, which are denoted without the ‘M’ lower suffix, the second order truncated expression for the strain energy of the macromodel can be obtained in the quadratic form

$$\Phi(\mathbf{E}, \mathbf{d}, \nabla \mathbf{d}) \cong \frac{1}{2} (\mathbf{S} \cdot \mathbf{E} + \mathbf{z} \cdot \mathbf{d} + \mathbf{Z} \cdot \nabla \mathbf{d}), \quad (13)$$

where the linearized stress measures,  $\mathbf{S}$ ,  $\mathbf{z}$ ,  $\mathbf{Z}$ , are derived as

$$\begin{aligned}\mathbf{S} &= \frac{\partial \Phi(\mathbf{E}, \mathbf{d}, \nabla \mathbf{d})}{\partial \mathbf{E}} = \mathbf{A} \mathbf{E} + \mathbf{C} \mathbf{d} + \mathbf{D} \nabla \mathbf{d} \\ \mathbf{z} &= \frac{\partial \Phi(\mathbf{E}, \mathbf{d}, \nabla \mathbf{d})}{\partial \mathbf{d}} = \mathbf{I} \mathbf{E} + \mathbf{M} \mathbf{d} + \mathbf{N} \nabla \mathbf{d} \\ \mathbf{Z} &= \frac{\partial \Phi(\mathbf{E}, \mathbf{d}, \nabla \mathbf{d})}{\partial \nabla \mathbf{d}} = \mathbf{O} \mathbf{E} + \mathbf{Q} \mathbf{d} + \mathbf{R} \nabla \mathbf{d} .\end{aligned}\quad (14)$$

It is worth noting that the material hyperelasticity entails symmetry relations between the components of the pairs of tensors  $(\mathbf{C}, \mathbf{I})$ ,  $(\mathbf{D}, \mathbf{O})$ ,  $(\mathbf{N}, \mathbf{Q})$ . Moreover, if the material microstructure is arranged by respecting the central symmetry, as in the case of any periodical microstructure, the odd order tensors  $\mathbf{C}$ ,  $\mathbf{I}$ ,  $\mathbf{N}$ ,  $\mathbf{Q}$  are null [10].

### 2.2.2. Identification of the constitutive function for the inertial actions

In this section we use the equivalence procedure to identify the inertial terms of the external actions of the continuum. Taking into account Eqs. (6) with the internal constraint (7), the mean work of the inertial actions of the module, Eq. (4), can also be written, after some algebra, in terms of  $\mathbf{u}$ ,  $\mathbf{W}$ ,  $\mathbf{d}$  and their gradients

<sup>10</sup> In some earlier papers of the Authors ([12], [28]), according to the formulation of the classical molecular theory of elasticity [31], [34], the identification procedure was based on the equivalence of the intermolecular potential and the continuum strain energy. This approach requires the selection of the response functions for the lattice internal actions to derive the stress measures of the macromodel.

$$\begin{aligned} \bar{\mathbf{w}}_{\mu}^e(\mathbf{u}, \mathbf{W}, \mathbf{d})^{\text{N}} = & -\frac{1}{V} \left\{ \left[ \sum_a \rho^a \ddot{\mathbf{u}}^a + \sum_h \rho^h \ddot{\mathbf{u}}_p^h \right] \cdot \mathbf{u} + \left[ \sum_a \rho^a \ddot{\mathbf{u}}^a \otimes (\mathbf{a} - \mathbf{x}) + \sum_h \rho^h \ddot{\mathbf{u}}_p^h \otimes (\mathbf{p}^h - \mathbf{x}) \right] \cdot \nabla \mathbf{u} \right. \\ & \left. + \frac{1}{2} \sum_a \mathbf{A}^a \cdot \mathbf{W} + \sum_h \rho^h \ddot{\mathbf{d}}^h \cdot \mathbf{d} + \sum_h \rho^h \ddot{\mathbf{d}}^h \otimes (\mathbf{h} - \mathbf{x}) \cdot \nabla \mathbf{d} \right\}. \end{aligned} \quad (15)$$

Evaluating the total external work of the module on  $\mathcal{M}$  and then applying the divergence theorem yields

$$\begin{aligned} \mathbf{w}_{\mu}^e(\mathbf{u}, \mathbf{W}, \mathbf{d})^{\text{N}} = & \int_{\mathcal{M}} \bar{\mathbf{w}}_{\mu}^e{}^{\text{N}} dV = \int_{\mathcal{M}} \mathbf{b}_{\mu}^{\text{N}} \cdot \mathbf{u} dV + \frac{1}{2} \int_{\mathcal{M}} \mathbf{B}_{\mu}^{\text{N}} \cdot \mathbf{W} dV + \int_{\mathcal{M}} \mathbf{g}_{\mu}^{\text{N}} \cdot \mathbf{d} dV \\ & + \int_{\partial \mathcal{M}} \mathbf{f}_{\mu}^{\text{N}} \cdot \mathbf{u} dA + \frac{1}{2} \int_{\partial \mathcal{M}} \mathbf{M}_{\mu}^{\text{N}} \cdot \mathbf{W} dA + \int_{\partial \mathcal{M}} \mathbf{h}_{\mu}^{\text{N}} \cdot \mathbf{d} dA, \end{aligned} \quad (16)$$

with the body actions defined by the relations

$$\begin{aligned} \mathbf{b}_{\mu}^{\text{N}} = & -\frac{1}{V} \left\{ \sum_a \rho^a \left\{ \ddot{\mathbf{u}}^a - \text{div}[\ddot{\mathbf{u}}^a \otimes (\mathbf{a} - \mathbf{x})] \right\} + \sum_h \rho^h \left\{ \ddot{\mathbf{u}}_p^h - \text{div}[\ddot{\mathbf{u}}_p^h \otimes (\mathbf{p}^h - \mathbf{x})] \right\} \right\}, \\ \mathbf{B}_{\mu}^{\text{N}} = & -\frac{1}{V} \sum_a \mathbf{A}^a, \\ \mathbf{g}_{\mu}^{\text{N}} = & -\frac{1}{V} \sum_h \rho^h \left\{ \ddot{\mathbf{d}}^h - \text{div}[\ddot{\mathbf{d}}^h \otimes (\mathbf{h} - \mathbf{x})] \right\}, \end{aligned} \quad (17)$$

and the surface tractions

$$\begin{aligned} \mathbf{f}_{\mu}^{\text{N}} = & -\frac{1}{V} \left[ \sum_a \rho^a \ddot{\mathbf{u}}^a \otimes (\mathbf{a} - \mathbf{x}) + \sum_h \rho^h \ddot{\mathbf{u}}_p^h \otimes (\mathbf{p}^h - \mathbf{x}) \right] \mathbf{n}, \\ \mathbf{M}_{\mu}^{\text{N}} = & \mathbf{0}, \\ \mathbf{h}_{\mu}^{\text{N}} = & -\frac{1}{V} \sum_h \rho^h \ddot{\mathbf{d}}^h \otimes (\mathbf{h} - \mathbf{x}) \mathbf{n}, \end{aligned} \quad (18)$$

where  $\mathbf{n}$  is the outward normal to  $\partial \mathcal{M}$ . Finally, considering the constrained homogeneous deformations also for the accelerations, that is substituting Eqs. (6) and (7) into Eqs. (17) and (18), and neglecting infinitesimal terms of order higher than  $\nabla \mathbf{u}$  and  $\nabla \mathbf{d}$ , one has,

$$\begin{aligned} \mathbf{b}_{\mu}^{\text{N}} = & -\frac{1}{V} (\sum_a \rho^a + \sum_h \rho^h) \ddot{\mathbf{u}} = -\rho \ddot{\mathbf{u}}, \\ \mathbf{B}_{\mu}^{\text{N}} = & -\frac{1}{V} \sum_a [\mathbf{E}^a (\dot{\mathbf{W}} + \mathbf{W}^2)^{\text{T}} - (\dot{\mathbf{W}} + \mathbf{W}^2) \mathbf{E}^a], \\ \mathbf{g}_{\mu}^{\text{N}} = & -\frac{1}{V} \sum_h \rho^h \ddot{\mathbf{d}} = -\mu \ddot{\mathbf{d}}, \end{aligned} \quad (19)$$

and, considering  $\mathbf{x}$  as the centre of  $\mathcal{M}$ ,

$$\begin{aligned}
\mathbf{f}_\mu^{\text{IN}} &= -\frac{1}{V} \nabla \ddot{\mathbf{u}} \left[ \sum_a \rho^a (\mathbf{a} - \mathbf{x}) \otimes (\mathbf{a} - \mathbf{x}) + \sum_h \rho^h (\mathbf{p}^h - \mathbf{x}) \otimes (\mathbf{p}^h - \mathbf{x}) \right] \mathbf{n} = \mathbf{S}_\mu^{\text{IN}} \mathbf{n}, \\
\mathbf{M}_\mu^{\text{IN}} &= \mathbf{0}, \\
\mathbf{h}_\mu^{\text{IN}} &= -\frac{1}{V} \nabla \ddot{\mathbf{d}} \sum_h \rho^h (\mathbf{h} - \mathbf{x}) \otimes (\mathbf{h} - \mathbf{x}) \mathbf{n} = \mathbf{Z}_\mu^{\text{IN}} \mathbf{n},
\end{aligned} \tag{20}$$

By identifying the inertial external work of the module (micro-work), Eq. (16), with the (macro) work of a multifield continuum under the inertial linearized actions  $\mathbf{b}^{\text{IN}}$ ,  $\mathbf{B}^{\text{IN}}$ ,  $\mathbf{g}^{\text{IN}}$ , in any corresponding linear field  $\mathbf{u}$ ,  $\mathbf{W}$ ,  $\mathbf{d}$ ,

$$\mathcal{W}_\mu^e(\mathbf{u}, \mathbf{W}, \mathbf{d})^{\text{IN}} = \mathcal{W}_M^e(\mathbf{u}, \mathbf{W}, \mathbf{d})^{\text{IN}} = \int_{\mathcal{M}} \mathbf{b}^{\text{IN}} \cdot \mathbf{u} dV + \frac{1}{2} \int_{\mathcal{M}} \mathbf{B}^{\text{IN}} \cdot \mathbf{W} dV + \int_{\mathcal{M}} \mathbf{g}^{\text{IN}} \cdot \mathbf{d} dV, \tag{21}$$

we obtain  $\mathbf{b}^{\text{IN}} = \mathbf{b}_\mu^{\text{IN}}$ ,  $\mathbf{B}^{\text{IN}} = \mathbf{B}_\mu^{\text{IN}}$ ,  $\mathbf{g}^{\text{IN}} = \mathbf{g}_\mu^{\text{IN}}$ . This equivalence implies vanishing of the resulting surface tractions  $\mathbf{S}_\mu^{\text{IN}} = \mathbf{0}$ ,  $\mathbf{Z}_\mu^{\text{IN}} = \mathbf{0}$ , which corresponds to the introduction of the further internal constraints  $\nabla \ddot{\mathbf{u}} = \mathbf{0}$ ,  $\nabla \ddot{\mathbf{d}} = \mathbf{0}$ .

It can be noted finally, that the same equivalence procedure can be used to derive the non inertial actions as trivial averages of the actions over the module.

### 3. THE BALANCE EQUATIONS OF THE MULTIFIELD CONTINUUM

The constitutive equations for the internal and the inertial actions derived using the above equivalence procedure in terms of virtual work are those of a multifield continuum characterized by the homogeneous kinematical fields  $\mathbf{u}$  and  $\mathbf{d}$  introduced in Eqs. (6) and by the field  $\mathbf{W}$  constrained as in Eq. (7). Due to the presence of additional field descriptors than the classical ones we have called it a multifield continuum.<sup>11</sup> As already introduced,  $\mathbf{u}$  represents the standard displacement vector field while  $\mathbf{d}$  and  $\mathbf{W}$  represent the non-standard displacement-jump and rotational fields, respectively. The linearized strain measures of such a continuum are the symmetric part of the standard displacement gradient,  $\mathbf{E}$ , plus the fields  $\mathbf{d}$  and  $\nabla \mathbf{d}$ .

The linearized stress measures, corresponding in the sense of mechanical work to these strain measures, are  $\mathbf{S}$ , the standard Cauchy stress tensor;  $\mathbf{z}$ , the internal volume force related to the presence of the microcracks, and  $\mathbf{Z}$ , the micro-stress tensor. More generally,  $\mathbf{z}$  is an auto-force that plays the role of a configurational force responsible of the internal changes of the system configuration [49], [50].

The stress-strain relationships of the linear model, which takes into account the central symmetry of any material with periodic microstructure, reduce to

$$\begin{aligned}
\mathbf{S} &= \mathbf{A} \mathbf{E} + \mathbf{D} \nabla \mathbf{d} \\
\mathbf{z} &= \mathbf{M} \mathbf{d} \\
\mathbf{Z} &= \mathbf{O} \mathbf{E} + \mathbf{R} \nabla \mathbf{d},
\end{aligned} \tag{22}$$

<sup>11</sup> A mechanical theory of such continua has been presented by Capriz [41]. Micromorphic continua, among them second gradient, microstretch, micropolar material, etc. [42] are special cases of multifield materials.

where the elastic fourth order tensors,  $\mathbf{A}$ ,  $\mathbf{D}$ ,  $\mathbf{O}$ ,  $\mathbf{R}$ , and the second order tensor  $\mathbf{M}$ , have components identified as described in Section 2.2.1. As mentioned above moreover, the material hyperelasticity entails the symmetry relation  $\mathbf{O} = \mathbf{D}^T$ .<sup>12</sup> This is the simplified constitutive model that we consider in the sequel.

According to the axiomatic description in [51], [52], in order to derive the balance equations of such a continuum<sup>13</sup> the virtual work of the external actions is required to coincide with the virtual internal work, i.e., one must have for any field  $\mathbf{u}$ ,  $\mathbf{d}$  and  $\nabla\mathbf{u}$ ,  $\nabla\mathbf{d}$ , when  $\mathbf{W}$  and  $\mathbf{E}$  are expressed as the skew-symmetric (7) and the symmetric part of  $\nabla\mathbf{u}$ , respectively. Thus,

$$\begin{aligned} \int_{\mathcal{M}} \mathbf{b} \cdot \mathbf{u} dV + \frac{1}{2} \int_{\mathcal{M}} \mathbf{B} \cdot \mathbf{W} dV + \int_{\mathcal{M}} \mathbf{g} \cdot \mathbf{d} dV + \int_{\partial\mathcal{M}} \mathbf{S} \mathbf{n} \cdot \mathbf{u} dA + \int_{\partial\mathcal{M}} \mathbf{Z} \mathbf{n} \cdot \mathbf{d} dA + \\ = \int_{\mathcal{M}} (\mathbf{S} \cdot \mathbf{E} + \mathbf{z} \cdot \mathbf{d} + \mathbf{Z} \cdot \nabla\mathbf{d}) dV, \end{aligned} \quad (23)$$

where the body actions include, in principle, both inertial and non inertial terms  $\mathbf{b} = \mathbf{b}^{\text{IN}} + \mathbf{b}^{\text{NI}}$ ,  $\mathbf{g} = \mathbf{g}^{\text{IN}} + \mathbf{g}^{\text{NI}}$ ,  $\mathbf{B} = \mathbf{B}^{\text{IN}} + \mathbf{B}^{\text{NI}}$ . By using the divergence theorem, and taking into account the constraint (7), the following momentum balance laws can be obtained

$$\begin{aligned} \text{div} \mathbf{S} + \mathbf{b}^{\text{NI}} &= \rho \ddot{\mathbf{u}}, \\ \mathbf{S} - \mathbf{S}^T + \mathbf{B}^{\text{NI}} &= -\mathbf{B}^{\text{IN}}, \\ \text{div} \mathbf{Z} - \mathbf{z} + \mathbf{g}^{\text{NI}} &= \mu \ddot{\mathbf{d}}, \end{aligned} \quad (24)$$

where  $\rho$  and  $\mu$  are the mass densities identified in Eqs. (19). Eq. (24a) represents the standard balance of linear momentum, Eq. (24b) the balance of angular momentum which, in case of null body couples, implies the symmetry of the standard stress tensor  $\mathbf{S}$ , and Eq. (24c) is the additional balance of linear momentum.

Moreover, since the strain descriptors,  $\mathbf{d}$  and  $\nabla\mathbf{d}$ , do not vanish under a rigid motion of the body and the internal work must be null under any rigid motion, the additional balance equation ensues

$$(\mathbf{z} \otimes \mathbf{d} - \mathbf{d} \otimes \mathbf{z}) + (\mathbf{Z} \nabla\mathbf{d}^T - \nabla\mathbf{d} \mathbf{Z}^T) = \mathbf{0}. \quad (25)$$

This equation is a further moment balance equation and must be satisfied for any field  $\mathbf{d}$  and  $\nabla\mathbf{d}$  and must be considered as an additional constitutive prescription for the continuous model.<sup>14</sup>

<sup>12</sup> The apex ‘T’ stands for the major transposition index such that:  $\mathbf{AA} \cdot \mathbf{B} = \mathbf{A} \cdot \mathbf{A}^T \mathbf{B}$  for any fourth order tensor  $\mathbf{A}$  and any pair of second order tensors  $\mathbf{A}$  and  $\mathbf{B}$ .

<sup>13</sup> In general for multifield continua the standard invariance theorems cannot be used to derive the full set of balance equations [53].

<sup>14</sup> In a previous paper of the authors [28], the stiffer internal constraint  $\mathbf{W} = \mathbf{0}$  was considered instead of (7). This implies that the skew-symmetric part of the stress  $\mathbf{S}$  is equal to the left hand term of Eq. (25), so that it cannot be selected independently of the non-standard stress measures,  $\mathbf{z}$  and  $\mathbf{Z}$ , as it occurs herein. For a discussion see [54].

#### 4. WAVE PROPAGATION IN ONE-DIMENSIONAL MICROCRACKED BAR

In order to verify the ability of the simplified multifield model described above to account for the presence of the microstructure made of distributed fibres, with same local orientation, and distributed microcracks, we analyse wave propagation. Attention is focused on a one-dimensional model with internal and inertial actions identified through the multiscale equivalence procedure described in Section 2.

The reference system is a one-dimensional bar of length  $L$ , characterised by a uniform distribution of fibres and microcracks arranged according to the orthotetragonal symmetry.<sup>15</sup> Denoting with  $u$  and  $d$  the longitudinal components of the standard displacement vector  $\mathbf{u}$  and of the distributed/smearred opening-displacement vector  $\mathbf{d}$ , respectively, the constitutive relations for the stress measures (22) become

$$\begin{aligned} S &= A u' + D d' \\ z &= M d \\ Z &= O u' + R d' \end{aligned} \quad (26)$$

where  $A, D, O, R$  and  $M$  are the sole independent components of the constitutive tensors and  $D=O$ . In particular for the considered system,  $A=Y$ , the Young's modulus;  $R = nY/\rho_m \pi l$  and  $M = mY\rho_m/\pi l$ , where  $\rho_m$  is the microcrack density per unit module length,  $l$  is the microcrack length and  $n$  and  $m$  are constants depending on the number and arrangement of the microcracks in the module. The coupling term  $D$  also depends on the microcrack size and arrangement and on the elastic constants of the matrix.

The coupled equations of motion (24) for this two-field scalar problem, in the presence of only inertial actions, read<sup>16</sup>

$$\begin{aligned} \ddot{u} - \alpha^2 u'' - \beta d'' &= 0, \\ \ddot{d} - \varepsilon u'' - \varphi^2 d'' + \eta d &= 0, \end{aligned} \quad (27)$$

where  $\alpha^2=A/\rho$ ,  $\beta=D/\rho$ ,  $\varepsilon=O/\mu$ ,  $\varphi^2=R/\mu$  and  $\eta=M/\mu$ . From now on, we use for the continuum multifield model the term 'macro' to indicate standard quantities and the term 'micro' to indicate the additional quantities that account for the presence of the material microstructure. Then, we define the total displacement  $u_t = u+d$  representing the sum of the macro and the micro displacements.

##### 4.1. Free wave propagation

Denoting with  $x$  the co-ordinate of the bar axis and  $t$  the time variable, let us consider waves which propagate in the  $x$  direction with wave number  $k$  and angular frequency  $\omega$ . A general solution for  $u$  and  $d$  of the form

$$\begin{aligned} u &= u_0 \exp[i(kx - \omega t)], \\ d &= d_0 \exp[i(kx - \omega t)], \end{aligned} \quad (28)$$

is assumed, with  $d_0$  and  $u_0$  constant. Substitution of Eqs. (28) in Eqs.(27) gives

<sup>15</sup> In the framework of the pursued formulation, fibres with the same local rigid rotation are considered.

<sup>16</sup> The balance of angular momentum implies that the mass couple  $\mathbf{B}$  is null.

$$(\mathbf{Q} - c^2 \mathbf{I}) \mathbf{v} = \mathbf{0} , \quad (29)$$

where  $c = \omega/k$ ,  $\mathbf{I}$  is the identity tensor and the components of the vector  $\mathbf{v}$  and the tensor  $\mathbf{Q}$  are

$$\{\mathbf{v}\} = \{u \ d\}^T , \quad [\mathbf{Q}] = \begin{bmatrix} \alpha^2 & \beta \\ \varepsilon & \varphi^2 + \eta/k^2 \end{bmatrix} . \quad (30)$$

A non trivial solution of the system (29) exists if the characteristic equation

$$(\alpha^2 - c^2)(\varphi^2 + \frac{\eta}{k^2} - c^2) - \beta\varepsilon = 0 \quad (31)$$

is satisfied. Tensor  $\mathbf{Q}$  plays the role of acoustic tensor of the multifield system; the positive square roots of its eigenvalues,  $c_u$ ,  $c_d$ , are the macro and micro wave velocities. In general, both these velocities depend on the wave number,  $k$ , and the system is dispersive. Note that if the terms  $\beta$  and  $\varepsilon$  are null, the corresponding equations of motion reduce to two uncoupled equations of macro and micro motion, respectively

$$\begin{aligned} \ddot{u} - \alpha^2 u'' &= 0 , \\ \ddot{d} - \varphi^2 d'' + \eta d &= 0 , \end{aligned} \quad (32)$$

where Eq. (32a) corresponds to the standard wave equation, satisfied by a macrowave propagating with constant macrovelocity while Eq. (32b) remains dispersive with velocity depending on the wave number or frequency (dispersion relation):

$$c_u = \alpha , \quad c_d = \sqrt{\varphi^2 + \frac{\eta}{k^2}} = \frac{\omega \varphi}{\sqrt{\omega^2 - \eta}} . \quad (33)$$

This situation occurs when no interactions between particles and slits ( $\mathbf{r}^{ah}$ ) are considered in the lattice model.

The solution of the multifield problem can be searched for as a superposition of waves propagating with different velocities depending on frequencies and material parameters. By way of example, let consider the superposition of two linear harmonic waves,  $u$  and  $d$ , of equal amplitude,  $u_0$ , different wave numbers,  $k_u$  and  $k_d$ , and different phase-velocities,  $c_u$  and  $c_d$ . Their superposition has the form

$$u_t = 2u_0 \sin \bar{k}(x - \bar{c}t) \cos \frac{\Delta k}{2}(x - c_g t) , \quad (34)$$

with  $\bar{k} = (k_u + k_d)/2$ ,  $\bar{c} = (c_u + c_d)/2$ ,  $\Delta k = k_u - k_d$ ,  $c_g = c_u - c_d$ .

Due to the dispersion properties the group velocity,  $c_g$ , generally differs from the average velocity,  $\bar{c}$ , and the shape of the resulting wave is altered. Physically, this seems to be a

consequence of partial reflections of waves occurring in encountering the microcracks (scattering). The presence of microcracks in the multifield model, represented by the additional field  $d$ , can then be interpreted as a disturbance spread along the bar that, differently from the classical continuum, alters the shape of travelling waves, depending on the microcrack density,  $\rho_m$ . In particular, for weakly damaged materials the disturbance is localised as in a beating-like phenomenon, Fig. (4a), while in highly damaged materials it spreads along the bar carried by the elastic wave, Fig. (4b). Consistent with physical expectations, the average velocity,  $\bar{c}$ , of the resulting wave decreases with the increase of the microcrack density, Fig. (5).

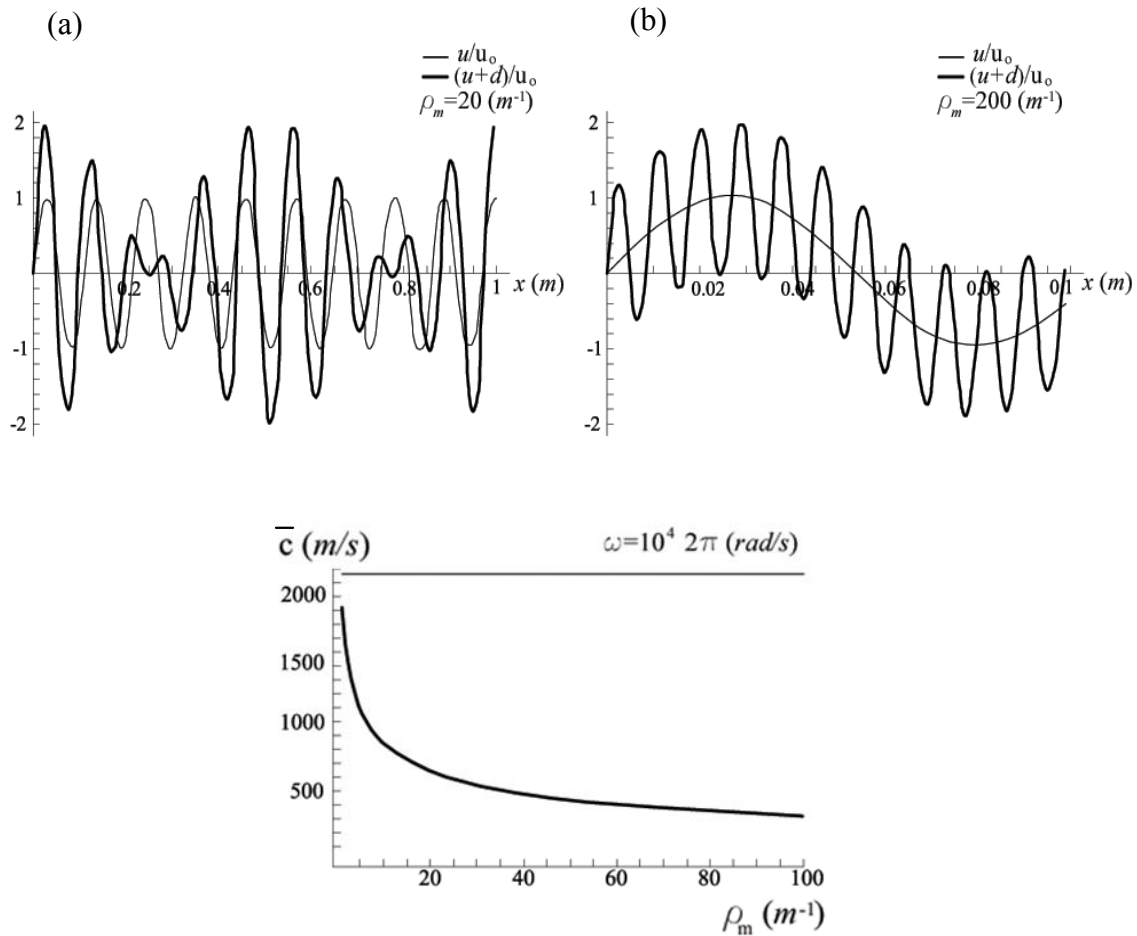


**Figure 5.** Phase-velocity vs microcrack density: elastic bar (thin); microcracked bar (thick).

#### 4.2. Forced waves: numerical simulations

In this Section the behaviour of forced waves in the one-dimensional model adopted is studied through numerical simulations. The uncoupled model obtained by putting  $\beta = \varepsilon = 0$ , whose equations of macro and micro motion in the absence of external body actions are Eqs. (32), is considered. The bar is simply supported and subjected to a sole cyclic axial force  $F(t) = F_0 \sin(\omega t)$  at the moving end ( $x = L$ ).

Coupling between micro and macro motion is taken into account by considering proper boundary conditions. With no body actions in fact, forced microwaves can only be produced by means of microforce boundary conditions. In general, when traction on a microcracked bar is

applied, it produces crack opening displacements that add to the standard displacement. Such a behaviour can be seen either as a consequence of the reduction of global stiffness (damage) or as an effect induced by an applied auto-force (microforce). Herein, this latter viewpoint is adopted, and both the macro and micro boundary conditions are set for this problem, respectively, as

$$\begin{aligned} u(0, t) = 0, & & d(0, t) = 0, \\ S(L, t) = F(t)/A, & \text{and} & Z(L, t) = \lambda F(t)/A. \end{aligned} \quad (35)$$

where  $A$  is the cross sectional area of the bar.

The axial microforce is herein identified in terms of the boundary macroforce via an energetic equivalence between a damaged bar, simulated by a finite number of longitudinal discontinuities, and an elastic bar with an additional force,  $AZ(L, t) = \lambda F(L, t)$ , with  $\lambda \geq 0$ . In turn the ratio  $\lambda$  between micro and macro boundary condition is assumed as depending on the material parameters of the microstructure, and specifically on the microcrack density per unit length,  $\rho_m$ . In particular,  $\lambda$  is obtained by linking the axial microforce  $AZ$  to the overall axial displacement of the discontinuities in the bar, each contribution being evaluated as the opening displacement of a slit in an elastic string with tension at infinity ([5], p. 117). This yields

$$\lambda = \frac{\rho_m}{2} \frac{1}{\pi}. \quad (36)$$

Relations (35) and (36) highlight that Neumann boundary conditions depend on constitutive prescriptions. The surface bounding of multifield continua cannot be regarded as a pure geometrical boundary, as for classical continua, but in a certain sense as a boundary having a mechanical substance. This result appears consistent with the generally non-trivial meaning of the boundary conditions in multifield problems [55]: think for instance of the reduction of the applied loads of a Saint-Venant's cylinder to generalized forces at the ends of a one-dimensional beam, in which the applied couples, playing the role of the present microforce, depend on the geometric characteristics of the cross section of the original 3D body.

In order to investigate the influence of the microscopic features of the material, we solve Eqs. (32) under the boundary conditions (35) by varying the microcrack density  $\rho_m$ . The numerical solutions are obtained by using the FEM based software COMSOL Multiphysics™, by directly implementing the multifield equations in a weak form.

Moreover, in order to explore the effects of this boundary action identification, two different assumptions are made concerning the coupling between micro and macro boundary conditions, namely:

- (i)  $\lambda$  varying with the microcrack density through Eq. (36);
- (ii)  $\lambda$  being constant with respect to  $\rho_m$ .

In the former case  $\rho_m$  affects both the constitutive parameter and the boundary conditions, in the latter it affects only the material parameters.

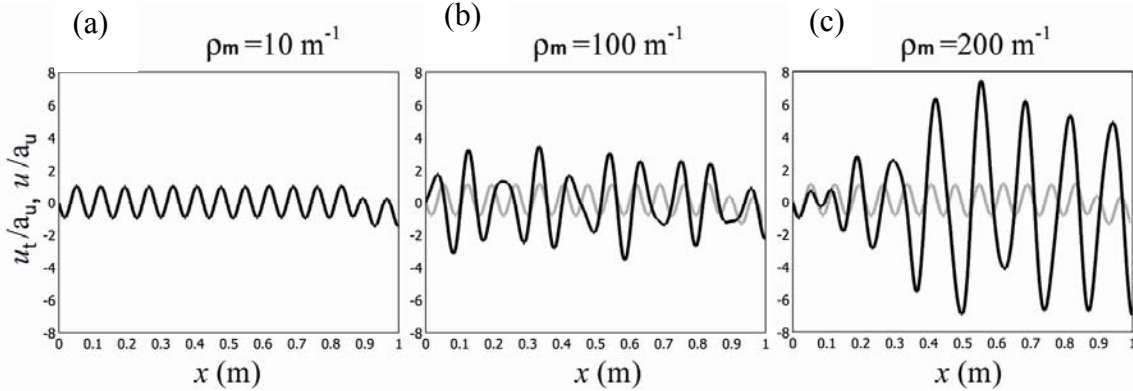
#### 4.2.1. The wave amplitude

Now, the effect of the micro-crack density on the amplitude of the resultant wave  $u_t = u + d$  is examined, using assumption (36).

In order to compare amplitudes, it is convenient to refer to the mean amplitude of resultant, macro and micro waves, defined as follows:

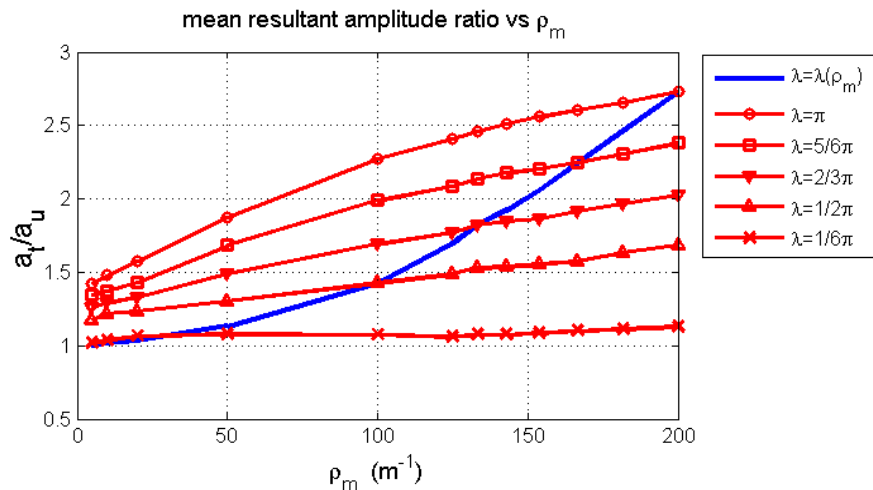
$$a_t = \left( \frac{2}{L} \int_0^L (u+d)^2 \right)^{\frac{1}{2}}; \quad a_u = \left( \frac{2}{L} \int_0^L u^2 \right)^{\frac{1}{2}}; \quad a_d = \left( \frac{2}{L} \int_0^L d^2 \right)^{\frac{1}{2}} \quad (37)$$

Figure 6 shows the resultant wave (thick line) for  $\rho_m = 10; 100; 200 \text{ m}^{-1}$  superposed on the macrowave (thin line), both being normalized with respect to the mean macro amplitude  $a_u$ . In the first case (low microcrack density, Fig. 6a) the amplitude of the microwave is so little that the resultant wave practically coincides with the macrowave. When the microcrack density increases, the effect of the microwave becomes more evident (Fig. 6b-c)



**Figure 6.** Macrowave in the elastic bar (thin line) and resulting wave in the damaged bar (thick line) for low (a), medium (b), high (c) microcrack density.

The dependence of the mean resultant amplitude on the microcrack density is summarized in Fig. 7 for the two different assumptions made above about the micro boundary conditions (assumption (i) is represented in blue, assumption (ii) in red).



**Figure 7.** Mean resultant amplitude ratio vs microcrack density.

In all of the examined cases the mean amplitude increases with the micro-crack density, by means of the constitutive relations. Yet, this dependency is strongly emphasized when properly linking  $\lambda$  to  $\rho_m$  through Eq. (36). In particular, the independency assumption (ii) has some

evident consequences: choosing a low value for  $\lambda$ , entails a really low ratio  $a_t/a_u$  for also high values of microcrack density, which corresponds to considerably underestimating the relevant effect on the overall amplitude of wave propagation. On the other hand, choosing a high  $\lambda$  value provides a significant ratio  $a_t/a_u$  also for low values of microcrack density. This means that for low values of  $\lambda$ , micro and macro waves are always incomparable, whereas for high values of  $\lambda$  they are comparable.

#### 4.2.2. The wave shape

The presence of dispersive waves with velocity depending on the frequency or wave number produces a distortion in the shape of the resulting waves, as already highlighted in the case of free oscillations (Section 4.1). In order to emphasize the distortion of wave shape due to the superposition of micro and macro waves and to show its dependence on the microcrack density, we define a “dummy resultant wave”, as follows:  $w = u/a_u + d/a_d$ .

In this way, summing waves of unit amplitude, we can compare the frequencies, irrespective of actual amplitudes.

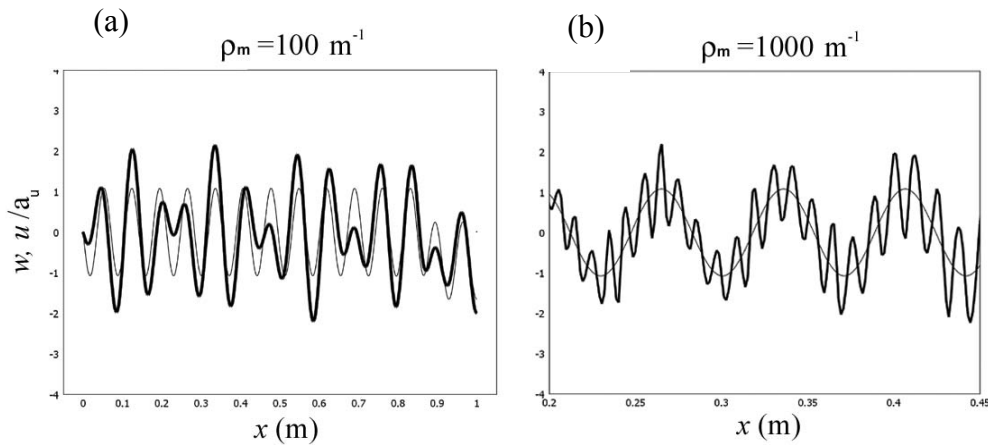


**Figure 8.** Macrowave in the elastic bar (thin line) and resulting wave in the damaged bar (thick line) for lower (a) and higher (b) microcrack density.

The results in Fig. 8 substantially confirm the wave scattering effect, already noticed in the free wave propagation, produced by the dispersion properties of the multifield model. The presence of microcracks alters the shape of travelling waves, depending on the microcrack density. In particular, the disturbance is localised for weakly damaged materials (Fig. 8a), while it spreads over the bar carried by the elastic wave for highly damaged materials (Fig. 8b).

## 5. FINAL REMARKS

A multiscale approach, first developed to grossly describe the mechanical behaviour of composite media, has been generalized within the framework of a molecular/energetic formulation of the theory of elasticity wherein changes in positions of specific lattice models, which account for the complex internal structure of a microcracked solid with embedded fibres, are related to the macroscopic deformations of a target multifield continuum. Upon describing the kinematics, dynamics and constitutive function of the micromodel, the constitutive relations for the internal and external (inertial) actions of the macromodel have been obtained via a

virtual work equivalence procedure. Referring to an internally constrained micromodel, the elastodynamic balance equations of the ensuing multifield continuum involve both standard (macro) and non-standard (micro) displacement vector fields as well as a microrotation vector field, thus allowing the complex dynamic interactions associated with the composite material microstructure to be taken into account. The derived multifield continuum naturally owes all the structural properties required by complex phenomenology, such as material internal lengths, dispersion properties and, as it could be easily shown, thermodynamic compatibility.

Thereafter, based on the considered modelling, elastic wave propagation in a microcracked one-dimensional bar has been addressed. Upon showing that the wave velocity decreases with the increase of microcrack density, in the free propagation problem, attention has been focused on forced waves for the case of uncoupled longitudinal macro and microdisplacement fields, though suitably coupled through boundary conditions. The ensuing fictitious microforce properly takes into account the system damage, represented by the microcrack density. Analysis of macro versus resultant (macro plus micro) waves in the undamaged/damaged bar has been accomplished in terms of the relevant amplitude and shape features via multifield finite element simulations. The microcracks play the role of a disturbance spread over the bar which alters the shape of travelling waves.

Overall, even in the solely indirectly coupled version herein considered, the multifield model shows to be able to describe the scattering of travelling waves associated with modifications of material properties. The classical continuum, lacking in dispersion properties, cannot reproduce this effect. This is a necessary prerequisite for studying the strain localization phenomena which often characterize the mechanical behaviour of brittle composite materials. In addition, based on the dispersion properties of such multifield continua, further developments are expected in the field of seismic wave propagation in fractured soils [56].

## 6. REFERENCES

- [1] D. C. Rapaport (1995), *The Art of Molecular Dynamics Simulation*, Cambridge University Press, Cambridge.
- [2] M. Rhee, H. M. Zbib, J. P. Hirth, H. Huang and T. de la Rubia (1998), Models for long/short range interactions and cross slip in 3D dislocation simulation of BCC single crystals, *Modeling & Simulation in Mater. Sci. & Engn.*, **6**, 467-492.
- [3] N. Pugno, A. Carpinteri, M. Ippolito, A. Mattoni and L. Colombo (2008), Atomistic fracture: QFM vs. MD, *Engineering Fracture Mechanics*, **75**, 1794-1803.
- [4] E. Sanchez-Palencia and A. Zaoui, Eds. (1985), Homogenization techniques for composite media, *Lecture Notes in Physics*, Vol. 272, Springer-Verlag, Berlin.
- [5] S. Nemat-Nasser and M. Hori (1993), *Micromechanics: Overall Properties of Heterogeneous Materials*, Elsevier, Amsterdam.
- [6] M. Ostoja-Starzewski, X. Du, Z.F. Khisaeva and W. Li (2007), Comparison of the size of the representative volume element in elastic, plastic, thermoelastic, and permeable random microstructures, in P. Trovalusci (Ed.), 'Multiscale Mechanical Modelling of Complex Materials and Engineering Application', *International Journal for Multiscale Computational Engineering*, **5**(2), 73-82.
- [7] M. Ostoja-Starzewski (2008), *Microstructural Randomness and Scaling in Mechanics of Materials*, Taylor & Francis, Boca Raton (FL).
- [8] G. Geymonat, G. Muller and N. Triantafyllidis (1993), Homogenization of non-linearly elastic materials, Microscopic bifurcation and macroscopic loss of rank-one convexity, *Archive for Rational Mechanics Analysis*, **122**, 231-290.
- [9] P. Ponte Castañeda and P. Suquet (1998), Nonlinear composites, *Advances in Applied Mechanics*, **34**, 171-303.
- [10] P. Trovalusci and R. Masiani (1996), Material symmetries of micropolar continua equivalent to lattices, *International Journal of Solids and Structures*, **36**(14), 2091-2108.

- [11] P. Trovalusci and R. Masiani (2003), Non-linear micropolar and classical continua for anisotropic discontinuous materials, *International Journal of Solids and Structures*, **40**(5), 1281-1297.
- [12] P. Trovalusci and R. Masiani (2005), A multi-field model for blocky materials based on multiscale description, *International Journal of Solids and Structures*, **42**, 5778-5794.
- [13] R. Muki and E. Sternberg (1965), The influence of couple-stresses on singular stress concentrations in elastic solids, *Zeitschrift für Angewandte Mathematik und Physik*, **16**, pp. 611-648.
- [14] C. B. Banks and M. Sokolowski (1968), On certain two-dimensional applications of the couple stress theory, *International Journal of Solids and Structures*, **4**, 15-29.
- [15] H. E. Read and G. A. Hegemier (1984), Strain softening of rock, soil and concrete – a review article, *Mechanics of Materials*, **3**, 271-294.
- [16] L. J. Sluys, R. de Borst and H.-B. Mühlhaus (1993), Wave propagation, localization and dispersion in a gradient-dependent medium, *International Journal of Solids and Structures*, **30**(9), 1153-1171.
- [17] V. P. Smyshlyaev and K. D. Cherednichenko (2000), On rigorous derivation of strain gradient effects in the overall behaviour of periodic heterogeneous media, *Journal of the Mechanics and Physics of Solids* **48**(6-7), 1325-1357.
- [18] V. G. Kouznetsova, M.G.D. Geers and W.A.M. Brekelmans (2004), Multi-scale second order computational homogenization of multi-phase materials: a nested finite element solution strategy. *Computer Methods in Applied Mechanics Engineering*, **193**, 5525- 5550.
- [19] M.E. Gurtin, (1965). Thermodynamics and the possibility of spatial interaction in elastic materials, *Archive for Rational Mechanics and Analysis*, **19**, 339–352.
- [20] M. Ostoja-Starzewski, S.D. Boccara and I. Jasiuk (1999), Couple-stress moduli and characteristic length of a two-phase composite, *Mechanics Research Communications*, **26** (4), 387–396.
- [21] S. Forest, F. Pradel and K. Sab (2001), Asymptotic Analysis of Heterogeneous Cosserat Media. *International Journal of Solids and Structures*, **38**, 4585-4608.
- [22] P. R. Onck (2002), Cosserat modelling of cellular solids, *Comptes Rendus Mecanique*, **330**, 717-722.
- [23] R. H. J. Peerlings and N. A. Fleck (2004), Computational evaluation of strain gradient elasticity constants, *International Journal for Multiscale Computational Engineering*, **2**(4), 599-619.
- [24] P. Trovalusci and G. Augusti (1998), A continuum model with microstructure for materials with flaws and inclusions, *Journal de Physique IV*, **8**: 383–390.
- [25] P. M. Mariano and P. Trovalusci (1999), Constitutive relations for elastic microcracked bodies: from a lattice model to a multifield continuum description, *International Journal of Damage Mechanics*, **8**, 153-173.
- [26] V. Sansalone and P. Trovalusci and F. Cleri (2006). Multiscale modelling of materials by a multifield approach: Microscopic stress and strain distribution in fiber-matrix composites, *Acta Materialia*, **54**(13), 3485–3492.
- [27] V. Sansalone and P. Trovalusci (2007), A numerical investigation of structure–property relations in fibre composite materials, in P. Trovalusci (Ed.), ‘Multiscale Mechanical Modelling of Complex materials and Engineering Applications’, *International Journal for Multiscale Computational Engineering*, **5**(2), 141-152.
- [28] P. Trovalusci and G. Rega (2007), Elastic waves in heterogeneous materials as in multiscale-multifield continua, *Proceedings of Estonian Academy of Science Physics Mathematics*, **56**(2), 100-107.
- [29] W. Voigt (1887), *Theoretische Studien über die Elastizitätsverhältnisse der Kristalle*. Abhandlungen der Gesellschaft der Wissenschaften zu Göttingen, **XXXIV**.
- [30] H. Poincaré (1892), *Leçons sur la Théorie de l’Elasticité*, Carré, Paris,
- [31] W. Voigt (1910), *Lehrbuch der Kristallphysik*, B.G. Teubner, Leipzig.
- [32] P. Trovalusci, D. Capecchi, G. Ruta (2009), Genesis of the multiscale approach for materials with microstructure, *Archive of Applied Mechanics*. (On line first: DOI 10.1007/s00419-008-0269-7).
- [33] A. Askar (1985(1943)), *Lattice Dynamical Foundation of Continuum Theories*, World Scientific, Singapore.
- [34] J. L. Ericksen (1977), ‘Special Topics in Elastostatics’, in C.-S. Yih (Ed.), *Advances in Applied Mechanics*, Vol. 17, Academic Press, New York, pp. 189-241.
- [35] A. Kunin (1982), *Elastic Media with Microstructure-I (One-dimensional Models)*, Springer-Verlag, Berlin.

- [36] M. Fago, R. L. Hayes, E. A. Carter and M. Ortiz (2004), Density-functional-theory-based local quasicontinuum method: Prediction of dislocation nucleation, *Physical Review B*, **70**, 100102.
- [37] S. G. Bardenhagen and N. Triantafyllidis (1994), Derivation of higher order gradient continuum theories in 2,3-D non-linear elasticity from periodic lattice models, *Journal of the Mechanics and Physics of Solids*, **42**, 111–139.
- [38] R. E. Miller and E. B. Tadmor (2002), The quasicontinuum method: Overview, applications and current directions, *Journal of Computer-Aided Materials Design*, **9**, 203-239.
- [39] P. Palla, M. Ippolito, S. Giordano, A. Mattoni and L. Colombo (2008), Atomistic approach to nanomechanics: concepts, methods, and (some) applications, in N. Pugno (Ed.) *The nanomechanics in Italy*, Transworld Research Network, Kerala (India), pp. 75-107.
- [40] J. D. Goddard (2008), From granular matter to generalized continuum, in G. Capriz and P. M. Mariano (Eds.), ‘Mathematical Models of Granular Matter’, *Lecture Notes in Applied Mathematics*, Vol. 1937, 1, pp. 1-20, Springer-Verlag, Berlin.
- [41] G. Capriz (1989), *Continua with Microstructure*, Springer-Verlag.
- [42] A.C. Eringen (1999), *Microcontinuum Field Theories*, New York, Springer-Verlag.
- [43] B. Svendsen (2001), On the continuum modeling of materials with kinematic structure, *Acta Mechanica*, **152**, 49-79.
- [44] G. Friesecke and F.Theil (2002), Validity and failure of the Cauchy-Born hypothesis in a two-dimensional mass-spring lattice, *Journal of Nonlinear Science*, **12**, 445-478.
- [45] J.L. Ericksen (2008), On the Cauchy-Born rule, *Mathematics and Mechanics of Solids*, **13**, 199-220.
- [46] M.G.D. Geers, V.G. Kouznetsova and W.A.M. Brekelmans (2005), Computational homogenization, *CISM lectures* (Online publication).
- [47] L. D. Landau and E. M. (1972), *Teoria dell'Elasticità*, Editori Riuniti, Roma, p.174.
- [48] A. Mattoni, L. Colombo and F. Cleri (2004), Atomistic study of the interaction between a microcrack and a hard inclusion in beta-SiC, *Physical Review Letters B*, **70**:094108, 2004.
- [49] G. Maugin, *Material Inhomogeneities in Elasticity*, Chapman & Hall, London, 1993.
- [50] M. E. Gurtin (2000), *Configurational Forces as Basis Concept of Continuum Physics*, Springer-Verlag, Berlin.
- [51] P. Germain (1973), The method of virtual power in continuum mechanics. Part II: Microstructure, *SIAM Journal of Applied Mathematics*, **25**, 556-575.
- [52] A. Di Carlo (1996), A non-standard format for continuum mechanics, in *Contemporary Research in the Mechanics and Mathematics of Materials*, R. C. Batra and M. F. Beatty Eds, CIMNE, Barcelona, 92-104.
- [53] M. E. Gurtin and P. Podio-Guidugli (1992), On the formulation of mechanical balance laws for structured continua, *Zeitschrift für Angewandte Mathematik und Physik*, **43** (1), 181-190.
- [54] P. Trovalusci, V. Varano (2009), Microcracked materials as non-simple continua, *Materials Science Forum*. In print.
- [55] G. Capriz and P. Podio-Guidugli (2002), Whence the boundary conditions in modern continuum physics?, *Atti dei Convegni Lincei*, **210**, Rome, pp. 19-42.
- [56] J. A. Hudson (1981), Wave speeds and attenuation of elastic waves in materials containing cracks, *Geophysical Journal of the Royal Astronomical Society*, **64**, 133-150.